

## Nonlinear effects due to gravity in a conical Hele-Shaw cell

José A. Miranda\*

*Laboratório de Física Teórica e Computacional, Departamento de Física, Universidade Federal de Pernambuco, Recife, PE 50670-901, Brazil*

(Received 19 October 2001; published 19 February 2002)

In this work we study the viscous fingering instability in a conical Hele-Shaw cell under the presence of gravity. We focus on understanding how the dynamical evolution of the fingering patterns is affected by the combined action of gravity and cell topology. Gravity-induced nonlinear effects are studied by a mode-coupling approach. Our results show that the interplay between gravity and cell topology leads to important effects, and profoundly modifies pattern evolution. We have found that the most dramatic consequences refer to finger tip behavior. Depending on the relative values of fluids' densities and viscosities, finger tip splitting reaches maximum intensity at well defined, preferred values of the cell opening angle. In fact, finger tip splitting can be completely replaced by finger tip sharpening as the cell angle is varied. Finger competition dynamics is also significantly changed: it is considerably enhanced (restrained) if the displaced fluid is more (less) dense.

DOI: 10.1103/PhysRevE.65.036310

PACS number(s): 47.20.Ma, 47.60.+i, 47.20.Ky, 47.54.+r

### I. INTRODUCTION

The Saffman-Taylor instability [1] arises at the interface separating two viscous fluids constrained to flow in the narrow gap between closed spaced parallel plates, a device known as the Hele-Shaw cell. The instability can be originated by the density difference between the fluids, when gravity is acting, or by pressure gradients, when the less viscous fluid displaces the more viscous one. The action of gravity and/or flow injection give rise to the formation of beautiful patterns, where fingerlike structures can compete and split at their tips [2].

The vast majority of both theoretical and experimental work on viscous fingering pattern formation analyze the development of the Saffman-Taylor instability when the flow takes place in *flat* Hele-Shaw cells, by considering rectangular [1,2] and radial [3,4] setups. A third possibility analyzes flow in a flat cell in which the sidewalls form a wedge of angle  $\theta_0$  [5,6]. Flow in wedge shaped cells bridges the behavior between rectangular and radial setups: the rectangular (radial) case corresponds to  $\theta_0=0$  ( $\theta_0=2\pi$ ). A great deal has been learned from such flat-cell studies, both from academic and practical points of view [1–6]. However, since viscous flow may occur on substrates of various complex shapes, it is of interest to study flow in *non-flat* Hele-Shaw cells, and examine the influence of the background space geometry on the growth of the two-fluid interface.

Recently, researchers started to systematically investigate the impact of cell geometry and topology on the Saffman-Taylor problem defined in *non-flat* Hele-Shaw cells [7–10]. These theoretical works explored a variety of unconventionally shaped cells, such as spherical [7,8], cylindrical [9], and conical [10]. Each of these unusual cell geometries present unique features leading to distinct physical effects, which deserve separate, in-depth analyses. It has been shown in Refs. [7–10] that background geometry/topology plays a ma-

major role in determining the shape of the evolving patterns. In spherical cells [7] finger tip splitting is regulated by the cell's *Gaussian* curvature, while in cylindrical cells [9] finger competition is controlled by the cylinder's *mean* curvature. It is worth noting that gravity-driven flow in a cylindrical Hele-Shaw cell has been investigated experimentally more than a decade ago by Zhao and Maher [11]. These studies [7–11] are not merely academic, in the sense that they introduce relevant geometrical and topological components into the theoretical framework of conventional Hele-Shaw flows [1–6]. Such components must be taken into consideration in more accurate descriptions of various viscous fingering related phenomena, associated with a number of industrial and manufacturing processes (pressure molding, coating of thin films, etc.) [12–15].

Viscous fingering in a conical Hele-Shaw cell (in the absence of gravity) has been examined in Ref. [10]. The conical cell presents distinguished geometrical and topological characteristics that makes it significantly different from flat, spherical or cylindrical cells. The Gaussian curvature of a cone vanishes everywhere, except at its apex where it is singular [16]. Consequently, the cone's Gaussian curvature is not a good parameter to describe fluid-fluid interface behavior. In addition, the cone's mean curvature is not constant, but changes with the distance from its apex. As a result the cone's mean curvature does not seem to be a good control parameter as well. As opposed to flow in spherical and cylindrical cells, topology rather than geometry is the key factor in determining the shape of the patterns in conical cells. As discussed in Ref. [10] the cell's topology can be conveniently described by the cone opening angle. Indeed, it has been verified [10] that interfacial patterns show a significant sensitivity to variations in the conical cell's opening angle.

In the present paper we study the influence of gravity in the development of fingering patterns in a conical Hele-Shaw cell. We consider the action of both gravity and fluid injection, and investigate interface dynamics as a function of the cone opening angle. We focus on the coupling between cell

\*Email address: jme@lftc.ufpe.br

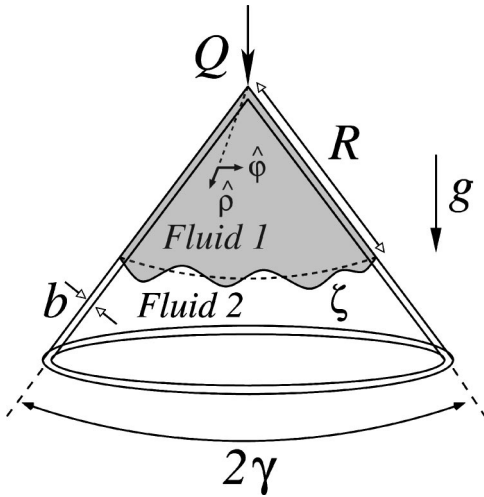


FIG. 1. Schematic configuration of flow in a conical Hele-Shaw cell under the action of gravity and injection. The cone opening angle  $0^\circ < 2\gamma \leq 180^\circ$ . Other relevant physical quantities are defined in the text. The unit vectors along the radial and azimuthal directions on the cone are represented by  $\hat{\rho}$  and  $\hat{\phi}$ , respectively.

topology and gravity, and study the consequences of such coupling to the nonlinear evolution of the emerging patterns. Throughout this work we will verify that gravity profoundly affects interface evolution.

The outline of the work is the following: Section II introduces our perturbative mode-coupling approach, and derives a nonlinear differential equation that governs the time evolution of the interface. Section III discusses the resulting motion. Section III A presents a brief discussion of the linear growth rate and identifies relevant stabilizing/destabilizing factors. Section III B uses the nonlinear mode-coupling differential equation to examine how gravity affects finger tip splitting and finger competition. The introduction of nonlinearity through gravity leads to important effects, and provide a much richer phenomenology. Section IV presents our final remarks and discusses perspectives of further study.

## II. FORMULATION AND MODE COUPLING

Consider the motion of two immiscible, incompressible, viscous fluids, flowing in a narrow gap between two coaxial, thin conical shells—the so-called *conical* Hele-Shaw cell (see Fig. 1). Both shells have the same opening angle  $2\gamma$  resulting in a constant gap thickness  $b$  between them. This geometrically constrained cell forces the flow to become essentially two dimensional, and the two-fluid interface one-dimensional. Therefore fluid flow takes place on the surface of a two-dimensional cone, embedded in three dimensions, described in polar coordinates  $(\rho, \varphi)$  by the metric

$$ds^2 = d\rho^2 + \rho^2 d\varphi^2, \quad (1)$$

where  $0 \leq \rho < \infty$  measures the distance along the surface of the cone from the apex  $\rho=0$ , and  $0 \leq \varphi \leq 2\pi\beta$  denotes the azimuthal angle measured on the cone, with  $0 < \beta \leq 1$ . If not by the change in the periodicity of  $\varphi$  metric (1) would describe an ordinary two-dimensional plane. Such unconven-

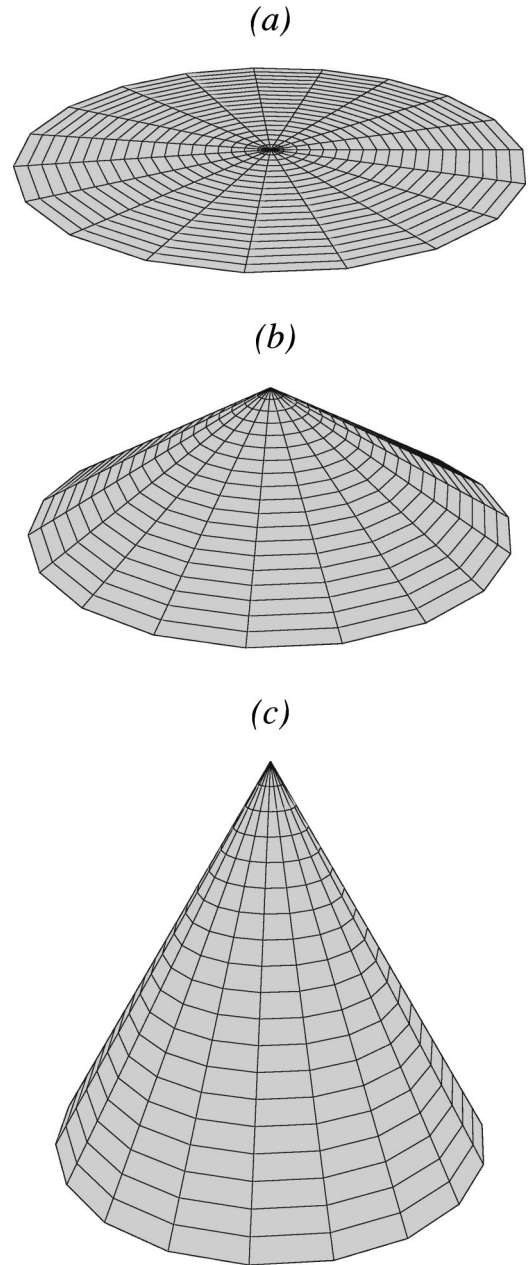


FIG. 2. Sketch of Hele-Shaw cells with (a)  $\beta=1$  (flat radial case,  $2\gamma=180^\circ$ ), (b)  $\beta=\sqrt{3}/2$  ( $2\gamma=120^\circ$ ), and (c)  $\beta=1/2$  ( $2\gamma=60^\circ$ ). The topological parameter  $\beta=\sin \gamma$ .

tional periodicity is intrinsically related to the conical nature of the background space on which the flow takes place.

The space defined by metric (1) describes a cone which is constructed by extracting a wedge of angle  $2\pi(1-\beta)$  from a planar surface, and by identifying the resulting edges. Such a cone is locally (but not globally) flat with a conical singularity at its vertex [16,17]. The Gaussian curvature of the cone is given by  $K=2\pi(1-\beta)\delta_2(\rho)$ , where  $\delta_2(\rho)$  is the two-dimensional delta function [18]. The parameter  $\beta$  measures the “sharpness” of the conical background space, as well as the intensity of the Gaussian curvature at the cone’s vertex. Note that  $\beta$  is conveniently related to the cone apex half angle by  $\beta=\sin \gamma$ . Figure 2 illustrates the general ap-

pearance of the Hele-Shaw cell for a few values of  $\beta$ . We use  $\beta$  to investigate how the nontrivial geometrical and topological features of the conical Hele-Shaw cell couple to gravity, and affect interfacial pattern formation.

The viscosities and densities of the upper and lower fluids are denoted as  $\eta_1$ ,  $\varrho_1$ , and  $\eta_2$ ,  $\varrho_2$ , respectively (Fig. 1). Fluid 1 is injected into fluid 2 through a small orifice located at the cone's vertex, at a given flow rate  $Q$ , which is the area covered per unit time. The flows are assumed to be irrotational and there is a surface tension  $\sigma$  between the fluids. The acceleration of gravity  $\mathbf{g}$  is constant, and points downwards along the cone's vertical axis of symmetry. During the flow, the two-fluid interface has a perturbed shape described as  $\rho \equiv \mathcal{R} = R + \zeta(\varphi, t)$ , where  $R = R(t)$  denotes the time dependent unperturbed radius and  $\zeta(\varphi, t)$  represents the interface perturbation amplitude. The unperturbed shape is a conical cap of radius  $R$  and surface area  $\mathcal{A} = \pi\beta R^2$ . Note the identity  $Q = vL$ , where

$$v = \frac{Q}{2\pi\beta R} \quad (2)$$

denotes the velocity of the unperturbed interface, and  $L$  is the unperturbed interface perimeter.

In order to investigate the dynamical evolution of the two-fluid interface in a conical Hele-Shaw cell, we represent the net interface perturbation as

$$\zeta(\varphi, t) = \sum_{n=-\infty}^{+\infty} \zeta_n(t) \exp\left(\frac{in\varphi}{\beta}\right), \quad (3)$$

where  $\zeta_n(t) = (1/2\pi\beta) \int_0^{2\pi\beta} \zeta(\varphi, t) \exp(-in\varphi/\beta) d\varphi$  denotes the complex Fourier mode amplitudes and  $n=0, \pm 1, \pm 2, \dots$  is the discrete azimuthal wave number.

The governing equation for the system is derived by adding a gravitational force term to a generalized version of the usual, flat Darcy's law [1,2], adjusted to describe flow in a conical Hele-Shaw cell [10], yielding

$$\begin{aligned} & A \left( \frac{\phi_1|_{\mathcal{R}^+} + \phi_2|_{\mathcal{R}}}{2} \right) - \left( \frac{\phi_1|_{\mathcal{R}^-} - \phi_2|_{\mathcal{R}}}{2} \right) \\ & = -\alpha\kappa|_{\mathcal{R}} + \chi\sqrt{1-\beta^2}\rho|_{\mathcal{R}}, \end{aligned} \quad (4)$$

where  $\phi_j$  defines the velocity potential in fluids  $j=1$  and  $2$ ,  $A = (\eta_2 - \eta_1)/(\eta_2 + \eta_1)$  is the viscosity contrast,  $\alpha = b^2\sigma/[12(\eta_1 + \eta_2)]$  contains the surface tension, and  $\chi = b^2g(\varrho_1 - \varrho_2)/[12(\eta_1 + \eta_2)]$  measures the strength of gravitational forces. To obtain Eq. (4) we used the pressure boundary condition  $p_1 - p_2 = \sigma\kappa|_{\mathcal{R}}$  at the interface  $\rho = \mathcal{R}$ , where  $\kappa$  is the interfacial curvature [2,10,19]. Note that the gravity term in Eq. (4) depends on  $\beta$ , and as expected, goes to zero in the flat-cell limit  $\beta \rightarrow 1$  (flat radial flow).

At this point, we would like to mention that the study of the Saffman-Taylor instability in conical cells allows one to investigate the action of gravitational forces in radially symmetric Hele-Shaw flows. Previous studies of radial source flow in flat, circular [3,4], and wedge shaped [5,6] cells do not include any contribution from gravity. Another interest-

ing point is the important qualitative distinction between gravity-driven flows in conical and inclined, rectangular Hele-Shaw cells [1,2]. In tilted rectangular cells, one may change the strength of the gravitational force by varying the cell's inclination angle with respect to the direction of  $\mathbf{g}$ . In rectangular cells, this can be done without varying the unperturbed flow velocity. In contrast, in conical cells both unperturbed velocity and gravitational force depend on  $\beta$ , and therefore are modified if the cone opening angle is varied. The connection of gravitational force and unperturbed velocity with  $\beta$  introduces interesting interfacial behavior.

To conclude our derivation, we follow standard steps performed in weakly nonlinear studies [7,10], by defining Fourier expansions for the velocity potentials, which obey Laplace's equation  $\nabla^2\phi_j = 0$ . We express  $\phi_j$  in terms of the perturbation amplitudes  $\zeta_n$  by considering the kinematic boundary condition  $\mathbf{n} \cdot \nabla\phi_1|_{\mathcal{R}} = \mathbf{n} \cdot \nabla\phi_2|_{\mathcal{R}}$ , where  $\mathbf{n}$  denotes the unit normal to the interface pointing from fluid 1 to fluid 2 [2,10,19]. Substituting these relations into Eq. (4), and Fourier transforming, yields the mode coupling equation of the Saffman-Taylor problem in a conical Hele-Shaw cell, taking into account both injection and gravity

$$\dot{\zeta}_n = \lambda(n)\zeta_n + \sum_{n' \neq 0} [F(n, n')\zeta_{n'}\zeta_{n-n'} + G(n, n')\dot{\zeta}_{n'}\zeta_{n-n'}], \quad (5)$$

where

$$\begin{aligned} \lambda(n) = & \left[ \frac{Q}{2\pi R^2\beta^2} (A|n| - \beta) - \frac{\alpha}{R^3\beta} |n| \left( \frac{n^2}{\beta^2} - 1 \right) \right. \\ & \left. + \frac{\chi}{R\beta} |n| \sqrt{1-\beta^2} \right] \end{aligned} \quad (6)$$

denotes the linear growth rate, and

$$\begin{aligned} F(n, n') = & \frac{|n|}{R} \left\{ \frac{QA}{2\pi R^2\beta^2} \left[ \frac{1}{2} - \text{sgn}(nn') \right] \right. \\ & \left. - \frac{\alpha}{R^3\beta} \left[ 1 - \frac{n'}{2\beta^2} (3n' + n) \right] \right\}, \end{aligned} \quad (7)$$

$$G(n, n') = \frac{1}{R} \left\{ A \frac{|n|}{\beta} [1 - \text{sgn}(nn')] - 1 \right\} \quad (8)$$

represent second-order mode coupling terms. The overdot denotes total time derivative, and the  $\text{sgn}$  function equals  $\pm 1$  according to the sign of its argument. It is worth noting that  $F(n, n')$  and  $G(n, n')$  depend on  $\beta$ , but show no dependence whatsoever on gravity. Gravitational forces will affect non-linear stages of interface evolution through the coupling of a full spectrum of modes, as expressed in Eq. (5).

### III. DISCUSSION

#### A. Linear growth rate

Before addressing the major subject of this work, namely the study of gravity-induced nonlinear effects in conical cells, we briefly discuss the linear growth rate expression (6). It is well known that the linear instability of the fluid-fluid interface can be evaluated by the sign of Eq. (6): if  $\lambda(n) > 0$  the disturbance grows, indicating instability.

We begin by describing each term in  $\lambda(n)$ . Inspecting Eq. (6) we observe the interplay of injection ( $Q$ ), surface tension ( $\alpha$ ), and gravity ( $\chi$ ) terms in determining the interface instability. In general, the injection term can be either positive or negative depending on the signs of  $Q$  and  $A$ . The case  $Q > 0$  ( $Q < 0$ ) corresponds to injection (suction) of fluid, while  $A > 0$  ( $A < 0$ ) is related to the case in which the upper (lower) fluid is the less viscous. The second term on the right hand side of Eq. (6) involves the contribution coming from surface tension, and clearly has a stabilizing nature ( $\sigma$  stabilizes modes of large  $n$ ). Finally, as a result of gravitational forcing the third term in Eq. (6) may be either positive or negative, depending on the relative values of the fluid's densities. If the upper fluid is more dense ( $\rho_1 > \rho_2$ ), gravity plays a destabilizing role. The opposite effect arises when  $\rho_1 < \rho_2$ .

On top of all these possible linear stability scenarios, note that the three terms in Eq. (6) contain an explicit dependence on unperturbed interface radius  $R$ , and on  $\beta$ . In general  $R$  is time dependent, so the balance among the various stabilizing/destabilizing terms depends on time, and their relative intensities may vary as the interface progresses. In addition, by virtue of its dependence on  $\beta$  the linear growth rate (6) would vary if the cell opening angle is modified. Because of the large number of independent parameters, even at the linear level, the study of the fluid-fluid interface dynamics in conical cells is not trivial.

To facilitate our analysis in the rest of the paper we will be concerned with the traditional experimental setup of the Saffman-Taylor problem, in which injection is positive  $Q > 0$ , and the less viscous fluid pushes the more viscous one, such that  $A > 0$ . Under these circumstances the first term in Eq. (6) is destabilizing, and even if gravity is neglected the viscosity contrast between the fluids may lead to complex interface shapes involving finger tip splitting and finger competition. To monitor gravitational effects we consider specific situations in which gravity can be either stabilizing or destabilizing. Within this scenario we systematically study how the coupling between gravity and cell topology influences growth in a conical cell. We carry out the nonlinear analysis of the system in the next sections.

#### B. Nonlinear effects

We use the mode coupling Eq. (5) to investigate how gravity influences the shape of the fingering patterns at the onset of nonlinear effects. We focus on the mechanisms of finger tip splitting and finger competition, and consider the coupling of a small number of modes. To simplify our discussion we rewrite Eq. (5) in terms of cosine and sine modes,

where the cosine  $a_n = \zeta_n + \zeta_{-n}$  and sine  $b_n = i(\zeta_n - \zeta_{-n})$  amplitudes are real valued. For consistent second order expressions, we replace the time derivative terms  $\dot{a}_n$  and  $\dot{b}_n$  by  $\lambda(n) a_n$  and  $\lambda(n) b_n$ , respectively. Without loss of generality we choose the phase of the fundamental mode so that  $a_n > 0$  and  $b_n = 0$ .

Finger tip splitting and tip sharpening phenomena are related to the influence of a fundamental mode  $n$  on the growth of its harmonic  $2n$  [20]. The equations of motion for the harmonic mode are written as

$$\dot{a}_{2n} = \lambda(2n)a_{2n} + \frac{1}{2}T(2n,n)a_n^2, \quad (9)$$

$$\dot{b}_{2n} = \lambda(2n)b_{2n}, \quad (10)$$

where the finger tip function is defined as

$$T(2n,n) = [F(2n,n) + \lambda(n)G(2n,n)]. \quad (11)$$

The function  $T(2n,n)$  controls finger tip behavior. The sign of  $T(2n,n)$  dictates whether finger tip splitting or finger tip sharpening is favored by the dynamics. If  $T(2n,n) < 0$ , the result is a driving term of order  $a_n^2$  forcing growth of  $a_{2n} < 0$ , the sign that is required to cause outwards pointing fingers to split. In contrast, if  $T(2n,n) > 0$  growth of  $a_{2n} > 0$  would be favored, leading to outward-pointing finger tip sharpening.

Finger competition is related to the influence of a fundamental mode  $n$ , assuming  $n$  is even, on the growth of its subharmonic mode  $n/2$  [20]. The equations of motion for the subharmonic mode are

$$\dot{a}_{n/2} = \left\{ \lambda(n/2) + \frac{1}{2}C(n/2)a_n \right\} a_{n/2}, \quad (12)$$

$$\dot{b}_{n/2} = \left\{ \lambda(n/2) - \frac{1}{2}C(n/2)a_n \right\} b_{n/2}, \quad (13)$$

where the finger competition function is defined as

$$C(n/2) = \left[ F\left(-\frac{n}{2}, \frac{n}{2}\right) + \lambda(n/2)G\left(\frac{n}{2}, -\frac{n}{2}\right) \right]. \quad (14)$$

The function  $C(n/2)$  disciplines finger competition. Observing Eqs. (12) and (13) we verify that  $C(n/2) > 0$  increases the growth of the cosine subharmonic  $a_{n/2}$ , while inhibiting growth of its sine subharmonic  $b_{n/2}$ . The result is an increased variability among the lengths of fingers of the less viscous fluid 1 penetrating into the more viscous fluid 2. This effect describes finger competition. Sine modes  $b_{n/2}$  would vary the lengths of fingers of the more viscous fluid 2 penetrating into the less viscous fluid 1, but it is clear from Eq. (13) that their growth is suppressed. Reversing the sign of  $C(n/2)$  would exactly reverse these conclusions, such that modes  $b_{n/2}$  would be favored over modes  $a_{n/2}$ . Regardless of its sign, the function  $C(n/2)$  measures the strength of the competition: increasingly larger values of  $C(n/2)$  lead to enhanced finger competition.

TABLE I. Experimental parameters used in situations I and II, taken from Refs. [1,3,4]. In situation I (II) fluid 1 is water (air) and fluid 2 is Shell Diala oil (glycerine). The acceleration of gravity  $g=980 \text{ cm/s}^2$ .

Situation	$\eta_1$ (g/cm s)	$\eta_2$ (g/cm s)	$\varrho_1$ (g/cm <sup>3</sup> )	$\varrho_2$ (g/cm <sup>3</sup> )	$\sigma$ (dyn/cm)	$b$ (cm)	$Q$ (cm <sup>2</sup> /s)
I	0.01	0.30	1.00	0.875	15	0.10	9.3
II	$\approx 0$	5.21	$\approx 0$	1.261	63	0.15	9.3

As pointed out in Sec. III A, the analysis of viscous fingering pattern formation in conical cells involves many independent parameters. Consequently, one must be particularly cautious in handling with situations in which the cell opening angle (or correspondingly,  $\beta$ ) is varied. We follow the instantaneous approach introduced in Ref. [7]: while  $\beta$  is varied, we look at the instantaneous tendency towards tip splitting and finger competition for interfaces of identical unperturbed  $v$  and  $L$ , taking advantage of the identity  $Q = vL$  [see Eq. (2)]. In the case of tip splitting, we consider a particular  $v$  and  $L$  combination at the onset of growth of mode  $2n$  [using the condition  $\lambda(2n)=0$ ] in the flat cell limit  $\beta \rightarrow 1$ , where it is known that  $T(2n,n)$  is negative [20]. In the analysis of finger competition, we take a different  $v$  and  $L$  pair at the onset of growth of mode  $n$  [using the condition  $\lambda(n)=0$ ] in the limit  $\beta \rightarrow 1$ , where it is known that  $C(n/2)$  is positive [20]. Using this approach we fix the  $(v, L)$  pairs that lead to the correct flat, radial flow behavior for which  $T(2n,n) < 0$  and  $C(n/2) > 0$ , and follow alterations in intensity and/or sign of these functions while  $\beta$  is varied.

Depending on the experimental parameters used, qualitatively different scenarios of interfacial instabilities can be considered in conical cells. In this work, we are interested in studying the effects of gravity in the usual viscosity-driven Saffman-Taylor instability. Therefore we set  $\eta_1 < \eta_2$ , and examine two different situations, regarding the relative values of the fluid's densities: (i) in situation I, water displaces oil. This is a rather typical situation [1] in which fluid 1 (water) is more dense and less viscous than fluid 2 (oil); (ii) in situation II, air is blown into glycerine. This is the usual configuration in viscous fingering experiments [3], where fluid 1 (air) is less viscous and less dense than fluid 2 (glycerine). The physical parameters we use in our calculations have been taken from classical experimental papers by Saffman and Taylor [1], Paterson [3], and Chen [4]. These parameters are presented in Table I.

### C. Situation I

First, let us examine situation I ( $\eta_1 < \eta_2, \varrho_1 > \varrho_2$ ). In this case the morphological instability can be driven by both viscosity and density differences between the fluids. We begin by examining tip splitting events. To illustrate how gravity affects tip splitting as a function of the cell opening angle, in Fig. 3 we plot  $T(2n,n)$  with respect to  $\beta$ , for two different values of mode number  $n$ . The solid black curves include gravitational driving, while the dashed gray curves neglect the effects of gravity. First, note that the black curves lie below the corresponding gray ones, meaning that gravity induces more negative values of  $T(2n,n)$ , and acts to favor

tendency toward tip splitting. This effect is not really surprising,  $\varrho_1 > \varrho_2$  and gravity is obviously a destabilizing factor. However, Fig. 3 quantifies important discrepancies between interface evolution in the presence/absence of gravity. If gravity is neglected, and we focus on a given mode  $n$ , we observe that the magnitude of  $T(2n,n)$  is maximum for the flat, radial case ( $\beta=1$ ) and monotonically decreases as  $\beta$  tends to zero. Therefore when gravity is neglected narrower cells would lead to less splitting.

On the other hand, when gravity is taken into account the behavior in Fig. 3 is considerably different: initially,  $T(2n,n) < 0$  decreases with decreasing  $\beta$ , reaches a minimum value, and subsequently increases as  $\beta$  tends to zero, although remaining always negative. The essential fact is that gravity not only leads to more splitting, but for each  $n$  it assigns a particular value of  $\beta$ , that we denote by  $\bar{\beta}(n)$ , at which  $T(2n,n)$  reaches a *minimum*. Consequently, for each mode  $n$  there is a specific value of the cone opening angle at which the intensity of finger tip splitting is strongest. This is an intrinsically nonlinear effect which is completely absent when gravity is neglected. Under the circumstances of situation I, one could control tip splitting and induce a certain number of split fingers, by setting the appropriate cell opening angle.

Figure 4 shows how  $\bar{\beta}(n)$  varies with mode  $n$ . By inspecting Fig. 4 we note that the values of  $\bar{\beta}(n)$  quickly drop to an asymptotic value  $\bar{\beta}(n \rightarrow \infty) \approx 0.7071$ , as  $n$  is increased. In Fig. 4  $\bar{\beta}(n \rightarrow \infty)$  is marked by a dashed line. For  $2 \leq n < \infty$ , the values of  $\beta$  that minimize  $T(2n,n)$  lie in a somewhat

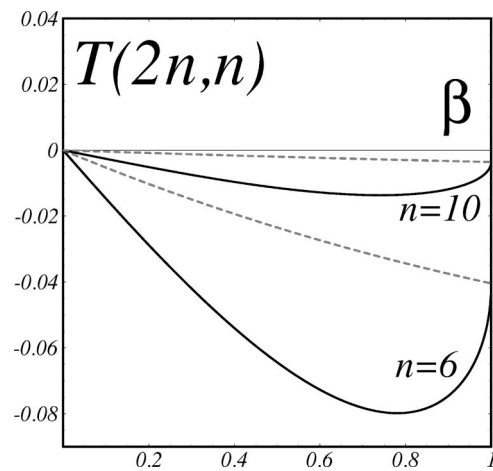


FIG. 3.  $T(2n,n)$  as a function of  $\beta$ , for modes  $n=6,10$  in situation I. The solid (dashed) curves describe evolution for nonzero (zero) gravity. The units of  $T(2n,n)$  are  $(\text{cm s})^{-1}$ .

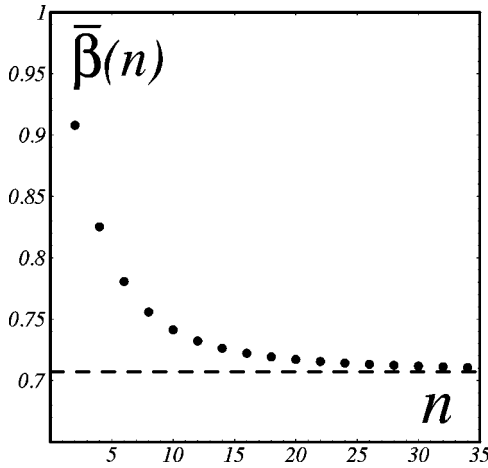


FIG. 4. Plot of  $\bar{\beta}(n)$  as a function of mode number  $n$ . The dashed line corresponds to the asymptotic value  $\bar{\beta}(n \rightarrow \infty) \approx 0.7071$ .

narrow range:  $0.7071 \leq \bar{\beta}(n) \leq 0.9080$ . In terms of the cone opening angle it corresponds to the interval  $90^\circ \leq 2\gamma \leq 130^\circ$ , which is actually small if compared to the total  $180^\circ$  range in  $2\gamma$ . This last finding is somehow unexpected, and could not be predicted from purely linear analysis. In practical terms, this narrow interval could be considered even narrower if we take into account the fact that the magnitude of  $T(2n, n)$  at  $\bar{\beta}(n)$  decreases very rapidly with increasing  $n$ , as can be easily verified in Fig. 3. Based on these conclusions we see that the inclusion of gravity in conical cells profoundly modifies pattern formation dynamics: finger tip splitting is strongest at a particular set of cell opening angles, concentrated within a narrow angular interval.

Still considering situation I, we investigate the effect of gravity on finger competition dynamics. Figure 5 illustrates how finger competition varies with the cell opening angle under the effect of gravity, and plots  $C(n/2)$  as a function of  $\beta$ . We contrast finger competition behavior in the presence of

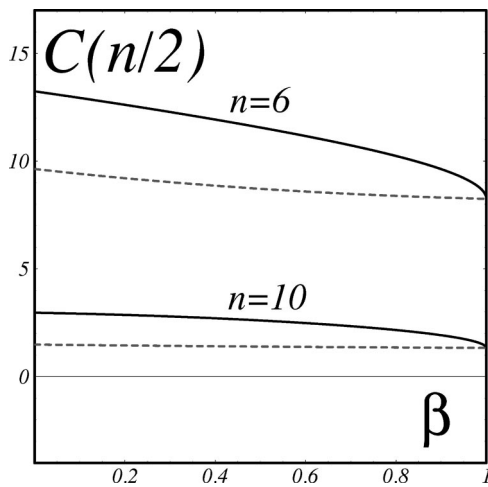


FIG. 5.  $C(n/2)$  as a function of  $\beta$ , for modes  $n=6, 10$  in situation I. The solid (dashed) curves describe evolution for nonzero (zero) gravity. The units of  $C(n/2)$  are  $(\text{cm s})^{-1}$ .

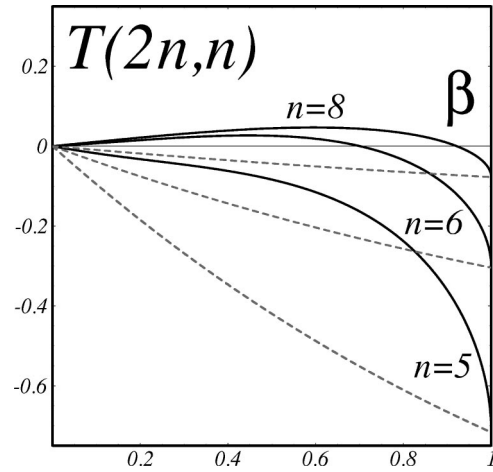


FIG. 6.  $T(2n, n)$  as a function of  $\beta$ , for modes  $n=5, 6$ , and  $8$  in situation II. The solid (dashed) curves describe evolution for non-zero (zero) gravity. The units of  $T(2n, n)$  are  $(\text{cm s})^{-1}$ .

gravity (solid black curves) with the case in which it is absent (dashed gray curves). The differences of results are not as dramatic as in the case of tip splitting events mentioned above, but are still noteworthy. We see from Fig. 5 that, all black curves lie above the gray ones, meaning that gravity enhances finger competition. As soon as  $\beta$  assumes values slightly smaller than 1, gravity takes over and competition increases significantly in comparison to the flat radial case ( $\beta=1$ ). Unlike finger tip splitting behavior, finger competition keeps increasing when  $\beta$  tends to zero.

#### D. Situation II

Now we turn our attention to situation II ( $\eta_1 < \eta_2, \varrho_1 < \varrho_2$ ). Recall that now the density of the displacing fluid 1 is smaller than the density of fluid 2. Consequently, gravity should play a stabilizing role. However, one should not forget that, as verified in situation I, nonlinearity may lead to important effects, and introduce a richer phenomenology. This is exactly what we find by examining tip splitting formation in situation II.

We start by analyzing Fig. 6, that shows how  $T(2n, n)$  varies with  $\beta$ , for  $n=5, 6$ , and  $8$ . Observing Fig. 6 we notice a remarkable feature: by varying  $\beta$  the function  $T(2n, n)$  changes not only its magnitude, but it also can reverse its sign. For mode  $n=5$  the black curve is above the dashed gray one, so gravity decreases the strength of tip splitting. Observe further that, for  $n=6$  and  $n=8$ ,  $T(2n, n)$  starts negative, but after reaching a critical value of  $\beta$  [calculated by setting  $T(2n, n)=0$ ], it becomes positive. We denote these values of  $\beta$  at which this “sign transition” in  $T(2n, n)$  occurs by  $\beta_c(n)$ .

The central result that can be extracted from Fig. 6 is that, if  $n > 5$  and  $\beta$  is decreased, gravity plays two distinct roles: it starts by inhibiting tip splitting, and after reaching  $\beta_c(n)$  it passes to favor tip sharpening. This is a legitimate signature of nonlinearity: gravity is linearly stabilizing ( $\varrho_1 < \varrho_2$ ), but in terms of tip sharpening formation it may play a destabilizing role. Obviously, this effect could not be predicted by linear stability analysis. Note in Fig. 6 that the zero-gravity,

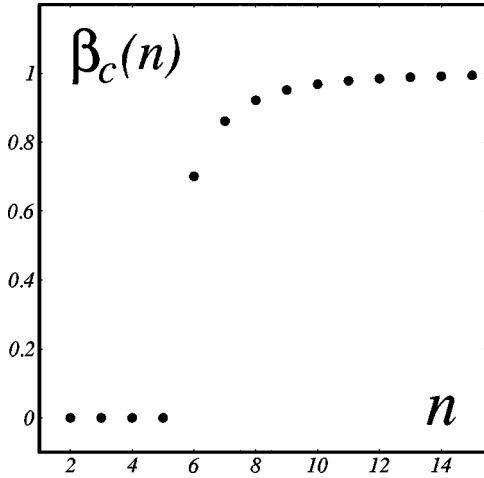


FIG. 7. Plot of  $\beta_c(n)$  as a function of mode number  $n$ . Note the abrupt change at  $n=6$ , corresponding to a “sign transition” in  $T(2n, n)$ .

dashed gray curves correspond to  $T(2n, n) < 0$  for all non-zero values of  $\beta$ . Therefore, if gravity is not taken into account, the interesting duality in the behavior of  $T(2n, n)$  mentioned above simply does not exist.

Figure 7 illustrates how the critical values  $\beta_c(n)$  vary with mode number  $n$ . For  $n < 6$  there is no change in the sign of  $T(2n, n)$  while  $\beta$  is decreased. At  $n=6$  there is a sudden jump in  $\beta_c(n)$ , meaning that at  $\beta_c(6) \approx 0.7008$  the tip splitting function is about to reverse its sign. We also note that  $\beta_c(n)$  tends asymptotically to 1 as  $n$  is increased. However, we should not expect dramatic transitions from tip splitting to tip sharpening when  $\beta \rightarrow 1$ , since the magnitude of  $T(2n, n)$  decreases with increasing  $n$ . The contribution of larger Fourier modes to finger tip splitting and tip sharpening is negligible. We estimate that the sign transition in  $T(2n, n)$  is more significant for modes  $6 \leq n \leq 10$ , where  $0.7008 \lesssim \beta_c(n) \lesssim 0.9680$ . In terms of the cone opening angle it corresponds roughly to the interval  $90 \lesssim 2\gamma \lesssim 150^\circ$ . Curiously, this interval of angles, in which interesting effects are more relevant in situation II, is very similar to the angular range in  $2\gamma$  that maximizes  $T(2n, n)$  in situation I. We lack an explanation for why this is so.

We conclude this section with a brief discussion about finger competition under the circumstances of situation II. In Fig. 8 we plot  $C(n/2)$  as a function of  $\beta$  for two different values of  $n$ . As a general observation, we see from Fig. 8 that nonzero gravity curves (solid) are all located below the zero-gravity ones (dashed). So, it is clear that gravity tends to suppress finger competition in comparison to the zero-gravity case.

A closer look at Fig. 8 reveals additional information. If gravity is neglected, we observe that the magnitude of  $C(n/2)$  is lowest in the flat, radial limit ( $\beta=1$ ), and increases monotonically as  $\beta$  tends to zero. The result is more competition for narrower cells. On the other hand, if gravity is present, the behavior of  $C(n/2)$  as a function of  $\beta$  is more subtle: unlike the zero-gravity case, competition is largest when  $\beta=1$ , progressively decreases as  $\beta$  is decreased, reaches a minimum, and then starts to increase very gently as

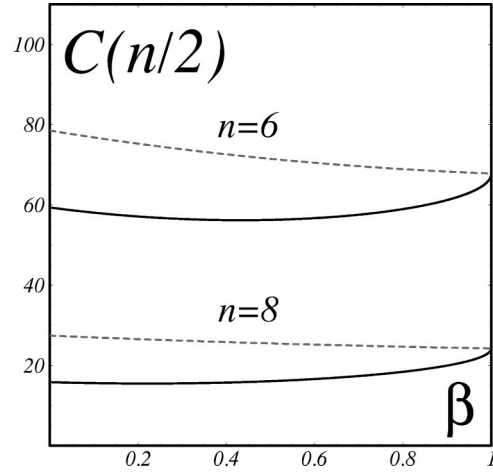


FIG. 8.  $C(n/2)$  as a function of  $\beta$ , for modes  $n=6, 8$  in situation II. The solid (dashed) curves describe evolution for nonzero (zero) gravity. The units of  $C(n/2)$  are  $(\text{cm s})^{-1}$ .

$\beta \rightarrow 0$ . For  $n=6$  ( $n=8$ ) the location of the minimum is  $\beta \approx 0.4331$  ( $\beta \approx 0.2210$ ). In fact, we have verified that the location of the minima tends very rapidly to  $\beta \approx 0$  as  $n$  is increased. In addition, the magnitude of  $C(n/2)$  at the minima decreases notably with increasing  $n$ . In principle, the coupling between gravity and cell topology could increase or decrease finger competition, depending on the value of the cell opening angle. However, based on the comments above, and on the behavior depicted in Fig. 8 we conclude that inhibition effects are much more significant. In practical terms, when gravity is acting the prevalent tendency of  $C(n/2)$  is to become lower and lower in magnitude as  $\beta$  is decreased.

#### IV. CONCLUSIONS AND PERSPECTIVES

In this paper we have investigated gravity-induced nonlinear effects in conical Hele-Shaw cells. We used a mode coupling approach to examine how gravity couples to cell topology and influences finger tip splitting and finger competition. Two basic situations have been considered: in situation I (II) the displacing fluid is less viscous and more (less) dense. In both situations we have found that the introduction of nonlinearity through gravity leads to important effects, with remarkable consequences for viscous fingering pattern formation.

The most dramatic consequences are related to finger tip behavior. In situation I gravity couples to cell topology to select specific values of the cell opening angle at which the strength of finger tip splitting is maximum for a given mode number  $n$ . In situation II, we have found that gravity plays a dual role: depending on the cell opening angle, and mode number  $n$  it may inhibit tip splitting, or favor tip sharpening. In this case, although gravity is linearly stabilizing, it may play a destabilizing role regarding tip sharpening phenomenon. With respect to finger competition we have found that the presence of gravity does not act as dramatically as in the tip-splitting case, but it still introduces significant changes in the magnitude of the effects: in situation I gravity considerably enhances competition among fingers, while in situation

It leads to a strong reduction in finger competition.

A couple of other important points related to gravity-driven flow in conical geometry still deserve to be investigated in more detail. The first one is the interesting possibility of avoiding the formation of finite time cusp singularities in the absence of surface tension. The role of rotation in the possible suppression of such singular behavior has been recently discussed by Magdaleno *et al.* [21], in the case of rotating, flat Hele-Shaw cells. In the conical cell case, the coupling between gravity and cell topology could possibly provide a similar kind of control over cusp instabilities. We can verify this point by inspecting the linear growth rate (6) in the zero surface tension case ( $\alpha=0$ ). In Eq. (6) we note that the injection term goes as  $1/R^2$ , while the gravity term varies as  $1/R$ . Since  $R$  is time dependent for  $Q \neq 0$ , the relative weight of injection and gravity terms determines which of the two effects dominates asymptotically in time. In fact, if  $Q > 0$ ,  $A > 0$ , and  $\varrho_1 > \varrho_2$ , the typical interface velocities decrease with increasing  $R$ , so gravity would dominate at long times. Under such circumstances, gravity could in principle, delay or even avoid cusp formation. It is worth noting that a similar kind of gravity-controlled effect can be obtained in spherical Hele-Shaw cells [8], where gravity would couple to cell's Gaussian curvature to prevent cusp formation. All these suggestive indications are of course based on linear theory, so its validity in fully nonlinear stages is still

an open question, and deserves a more complete and rigorous study.

It is also of interest to investigate in more detail the reasons why some of the most interesting behavior in conical cells with gravity happen at somewhat narrow range of opening angles. It would be of interest to verify the existence of a "critical angle," at which relevant nonlinear effects are more intense and dominant. This important issue has an interesting parallel with what has been observed in flat, wedge shaped cells. Experiments in the wedge geometry [5,6] observed an increasing sensitivity to finger tip splitting for larger angle  $\theta_0$ . Actually, there is some theoretical evidence [22] for the existence of a critical angle  $\theta_0 \approx 120-140^\circ$  in viscous fingering and diffusion-limited aggregation in wedge geometry. As claimed in Ref. [22], for wedges with an angle larger than  $\theta_0$  two split fingers could coexist without competition. Similar type of studies in conical cells could provide valuable information about the connection between dominant finger behavior and specific values of cell opening angles.

#### ACKNOWLEDGMENTS

I thank CNPq and FINEP (through its PRONEX Program) for financial support, and acknowledge useful discussions with Claudio Furtado.

- 
- [1] P. G. Saffman and G. I. Taylor, Proc. R. Soc. London, Ser. A **245**, 312 (1958).
  - [2] D. Bensimon, L. P. Kadanoff, S. Liang, B. I. Shraiman, and C. Tang, Rev. Mod. Phys. **58**, 977 (1986); G. Homsy, Annu. Rev. Fluid Mech. **19**, 271 (1987); K. V. McCloud and J. V. Maher, Phys. Rep. **260**, 139 (1995).
  - [3] L. Paterson, J. Fluid Mech. **113**, 513 (1981).
  - [4] J.-D. Chen, J. Fluid Mech. **201**, 223 (1989).
  - [5] H. Thomé, M. Rabaud, V. Hakim, and Y. Couder, Phys. Fluids A **1**, 224 (1989).
  - [6] E. Lajeunesse and Y. Couder, J. Fluid Mech. **419**, 125 (2000).
  - [7] F. Parisio, F. Moraes, J. A. Miranda, and M. Widom, Phys. Rev. E **63**, 036307 (2001).
  - [8] J. A. Miranda, F. Parisio, F. Moraes, and M. Widom, Phys. Rev. E **63**, 016311 (2001).
  - [9] J. A. Miranda, Phys. Rev. E **65**, 026303 (2002).
  - [10] J. A. Miranda and F. Moraes (unpublished).
  - [11] H. Zhao and J. V. Maher, Phys. Rev. A **42**, 5894 (1990).
  - [12] L. W. Schwartz and D. E. Weidner, J. Eng. Math. **29**, 91 (1995).
  - [13] A. Oron, S. H. Davis, and S. G. Bankoff, Rev. Mod. Phys. **69**, 931 (1997).
  - [14] S. Kalliadasis, C. Bielarz, and G. M. Homsy, Phys. Fluids **12**, 1889 (2000).
  - [15] J. A. Diez and L. Kondic, Phys. Rev. Lett. **86**, 632 (2001).
  - [16] M. P. do Carmo, *Differential Geometry of Curves and Surfaces* (Prentice Hall, New York, 1977).
  - [17] B. A. Dubrovin, A. T. Fomenko, and S. P. Novikov, *Modern Geometry-Methods and Applications, Parts 1 and 2* (Springer-Verlag, New York, 1984).
  - [18] D. M. Tavares and C. Romero, Mod. Phys. Lett. A **13**, 2077 (1998).
  - [19] L. D. Landau and E. M. Lifshitz, *Fluid Mechanics* (Pergamon, New York, 1987).
  - [20] J. A. Miranda and M. Widom, Physica D **120**, 315 (1998).
  - [21] F. X. Magdaleno, A. Rocco, and J. Casademunt, Phys. Rev. E **62**, R5887 (2000).
  - [22] D. A. Kessler, Z. Olami, J. Oz, I. Procaccia, E. Somfai, and L. M. Sander, Phys. Rev. E **57**, 6913 (1998).